Effective Hyperbolic Strain-Softened Shear Modulus for Driven Piles in Clay

Don C. Warrington, PhD, P.E., M.ASCE
University of Tennessee at Chattanooga
Departments of Civil and Mechanical Engineering

Presented at the University of Tennessee at Chattanooga Research Dialogues, 9-10 April 2019.

Although it is widely understood that soils are non-linear materials, it is also common practice to treat them as elastic, elastic-plastic, or another combination of states that includes linear elasticity as part of their deformation. Assuming hyperbolic behavior, a common way of relating the two theories is the use of strain-softened hyperbolic shear moduli. Applying this concept, however, must be done with care, especially with geotechnical structures where large stress and strain gradients take place, as is the case with driven piles. In this paper a homogenized value for strain-softened shear moduli is investigated for both shaft and toe resistance in clays, and its performance in the STADYN static and dynamic analysis program documented. A preliminary value is proposed for this "average" value based upon the results of the program and other considerations.

Keywords: pile capacity, soil shear modulus, hyperbolic strain softening, inverse methods

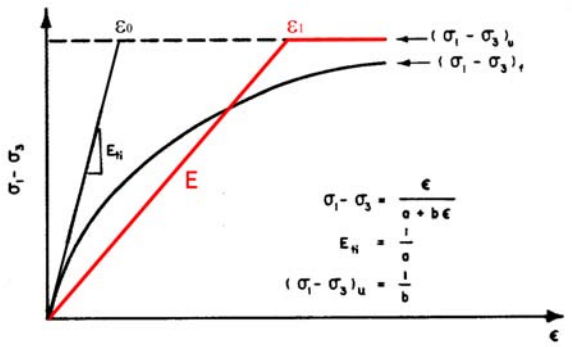

Figure 1. Hyperbolic Soil Model

Introduction

The non-linearity of soils is something that is better understood in principle than implemented in practice. Probably the most widely applicable nonlinear model of soils is the hyperbolic model, as presented by Duncan and Chang (1970). An illustration of this is shown in Figure 1.

Although this non-linearity is widely recognized, elastic and shear moduli are still used for actual engineering analysis. To be useful as a parameter to predict the stress-strain properties of the soil, the concept is to replace a gradually decreasing stress-strain Jacobian with a constant elastic modulus E which is maintained to the failure stress and a strain ϵ_1, at which point the soil responds in a plastic way.

At the beginning of deformation, the slope of the hyperbolic curve is the small-strain elastic modulus E_{ti}. If the material could maintain this modulus until failure, same would take place at the strain ϵ_0. This is referred to as the reference strain, and its importance will be demonstrated below. In reality the apparent elastic modulus progressively decreases with increasing strain. The hyperbolic model, however, implies either a decreasing secant or tangent modulus with increasing strain. The ratio of the small-strain modulus with the modulus at larger strains can be defined as follows:

$$\mu = \frac{E}{E_{ti}} \tag{1}$$

It should be apparent that the value of μ will decrease as the strain the soil experiences increases. Although there are qualitative ways of showing this to be so, at this point there is no really informative theoretical quantitative way of determining μ. Experimental data is certainly available for this and typical results are shown in Figure 2.

Figure 2 uses shear moduli and shear strain as opposed to elastic moduli and strain; these can be related to each other fairly easily. This means that the strain softening coefficient can also be defined as follows:

$$\mu = \frac{G}{G_0} \tag{2}$$

For most of this paper shear moduli and strain will be the focus as test data is more abundant for this than elastic moduli, but the concept is the same.

Figure 2 also illustrates another important point: the value of μ depends upon the nature of the loading and the degree of strain the material experiences. This varies with both the

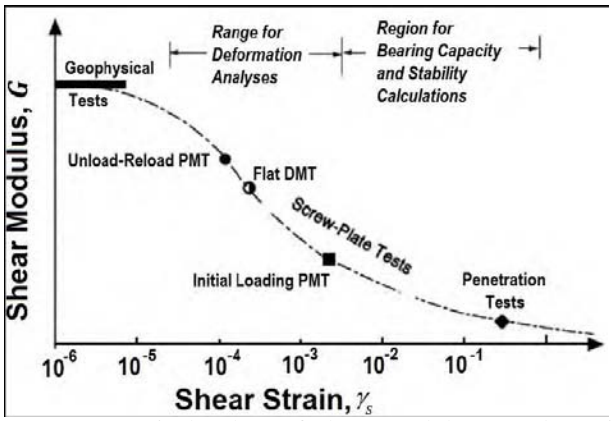

Figure 2. Typical Values of Shear Modulus Based on Field Tests (from Loehr, Lutenegger, Rosenblad, and Boeckmann (2016))

testing method and the type of loading a given soil experiences. Practitioners frequently use "typical" values of shear or elastic modulus in various calculations but these values should be informed by the application if not values of strain itself.

In this paper the following will be discussed:

1. Definition of the various constituents of the equation for both small-strain and large-strain shear moduli.

2. Estimation of an "average" value of μ for both shaft and toe elastic stress and strain.

3. Application of both of these to the STADYN program in both forward and inverse modes.

Shear Modulus Equation and Constituents

The basic expression for shear modulus in soils is expressed by the the following equation (Randolph, Dolwin, and Beck (1994)):

$$\frac{G_0}{p_{atm}} = S\,F\,(e)\left(\frac{\sigma_0}{p_{atm}}\right)^{\bar{n}} \tag{3}$$

This relationship appears in the literature in several forms, but it is important to formulate it in this way so that a) both sides of the equation are dimensionless and b) values for S in particular are independent of the units being used for a specific problem.

Combining this result with Equation 2 and rearranging yields the complete expression for shear modulus at a given strain level, thus

$$G = \mu S\,F\,(e)\left(\frac{\sigma_0}{p_{atm}}\right)^{\bar{n}} p_{atm} \tag{4}$$

Effective Stress Function

The main variation of the "effective stress" component $\left(\frac{\sigma_0}{p_{atm}}\right)^{\bar{n}}$ of Equation 4 is the value for $\bar{n}$, which varies from 0.4 to 0.6. For the purposes of this paper and others $\bar{n} = \frac{1}{2}$, which makes this component similar to a commonly used correction for SPT values for overburden. There are two important differences:

1. The SPT overburden correction factor is the inverse of this factor. The advantage of this for the current study is that the factor does not become unbounded when $\sigma_0 = 0$, although without some kind of lower limit the shear modulus at the soil surface is zero.

2. The soil stress used is not simply the vertical effective stress but the deviatoric stress,

$$\sigma_0 = \frac{\sigma_1 + \sigma_2 + \sigma_3}{3} \tag{5}$$

Void Ratio Function

The relationship between the shear modulus of a soil and its void ratio (or porosity) is well established and is demonstrated by Bui, Clayton, and Priest (2010). Although there are several formulations of this function, there are two which will be emphasized in this study.

The first is the classic formulation of Hardin and Black (1968). In a slightly simplified form, this is

$$F\,(e) = \frac{3 - e}{(1 + e)^2} \tag{6}$$

In terms of porosity, this is

$$F\,(n) = (n - 1)\,(4n - 3) \tag{7}$$

The main practical weakness of this formulation is that, for values of $e > 3$ or $n > \frac{3}{4}$, the function is negative. This problem can be avoided if the unified expression of Bui et al. (2010) is used, which is

$$F\,(e) = (1 + e)^{-3} \tag{8}$$

or

$$F\,(n) = (1 - n)^3 \tag{9}$$

While the formulation of Bui et al. (2010) solves many of these problems, it creates another one because $F\,(e)$ or $F\,(n)$ of Equations 8 and 9 cannot be blindly interchanged with those of Equations 6 and 7.

To understand this problem, consider the graphical comparison of Equations 6 and 8, shown in Figure 3.

It is easy to see that the two void ratio functions differ significantly in the lower range of void ratios where most soils exist. For the range of void ratios $0.5 < e < 1.5$, the ratio between Hardin and Black (1968) void ratio functions and Bui et al. (2010) void ratio functions do not vary a great deal, ranging from 3.75 to 4. Outside of that range the relationship of the two is much more complicated, although for very high void ratios both void ratio functions are both close and not very elevated. This is important because for this study

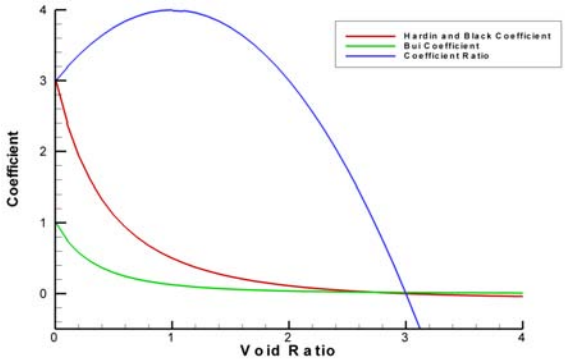

Figure 3. Comparison of Bui et al. (2010); Hardin and Black (1968) Coefficients vs. Void Ratio e

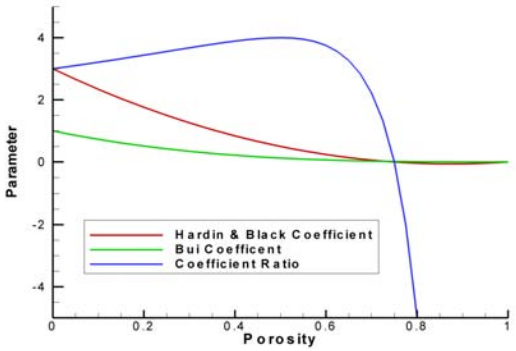

Figure 4. Comparison of Bui et al. (2010); Hardin and Black (1968) Coefficients vs. Porosity n

because ultimately the Bui et al. (2010) void ratio function will be used for the study, while much of the literature which features S is based on Hardin and Black (1968) type void ratio functions.

Another way to compare these functions is to compare the porosity functions, as shown in Figure 4.

Using porosity includes all possible value because $0 < n < 1$, while void ratio $0 < e < \infty$. This also shows that, for both functions, $F(n) = 0$ when $n = 1$, which makes sense.

Material Factor

Although the dependence of shear modulus on void ratio is due to the granular nature of the soils, the literature shows that this relationship widely varies not only with the void ratio function in use but also with the material itself. For example, Randolph et al. (1994) and Yang (2006) indicate that the coefficient $S_{H\&B}$ can vary from 400 for clean sands to 70 for silty sands. In general this coefficient decreases with increasing cohesion in soils due to their greater compressibility. Determining realistic, typical values for S is complicated not only by the usual variations in experimental data and methodologies but also by the fact that, as shown in Figure 3, the values used will depend upon the void ratio function employed.

Starting with the upper limit, using the $\xi - \eta$ continuum of Warrington (2016), the upper limit at $\eta = -1$ (cohesionless soils) can be set at $S_{H\&B} = 400$, which would translate to a maximum $1500 \leq S_{bui} \leq 1600$. While this is important, for the purposes of this study the lower limit is the more important. Bui et al. (2010) and Vardanega and Bolton (2013) indicate that, for clay soils at least, the value of S_{bui} can vary between 30 and 60 and sometimes can be lower with soft clays, using a void ratio function that is either similar or identical to Equation 8. For initial runs, testing very low values for S_{bui} resulted in some STADYN model collapse difficulties; these were resolved with a minimum $S_{bui} = 50$, which is in the range. In the interim, at $\eta = -1$, values of 100, 200 and 400 for S_{bui} were also evaluated, and these results are used to evaluate the overall performance of the model.

The variation of S_{bui} illustrates an important point: the product of the material factor S and the hyperbolic softening coefficient μ is a scalar. This means that their product is not a unique combination of the two. While in principle it is easy to separate the two in a controlled experimental environment, their use in actual practice is such that the same result for shear (and thus elastic) modulus can be obtain if, for example, S is raised and μ is lowered, and vice versa. This situation became an important aspect of this study.

Estimating a Range for the Hyperbolic Softening Coefficient

As mentioned earlier, the hyperbolic softening coefficient μ is not a constant for all applications but dependent upon the strain level experienced by the soil in a given application. In the case of driven piles (and deep foundations in general) this is complicated by very steep stress and strain gradients in the soil, which are at their highest adjacent to the pile (at the shaft or toe) and decrease fairly rapidly as one gets further away.

In a three-dimensional, continuum model such as STADYN (Warrington and Newman (2018),) one solution would be to vary the shear and elastic moduli as an element's (or integration point's) strain changes. While this may be implemented at some future stage of the program's development, at this point this solution will not be implemented due to its complexity.

Another solution would be to establish an effective "average" (or more accurately homogenized) softening coefficient and apply this to the entire model. Although not as exact as the first solution, this should give us a good working model while avoiding the complexity of the first proposed solution. At this stage the uncertainty of the parameters does not justify a more precise solution.

In establishing homogenized softening coefficients, two things must be considered, which to some extent contradict each other.

The first is that the goal is to simulate the elastic behavior of the soil. The simplest way to do this is to consider elastic solutions and adapt them to a varying shear or elastic modulus. Many of these solutions were developed mostly or entirely with a constant shear or elastic modulus, although Randolph and Wroth (1978) discuss the use of a variable shear modulus.

The second is that the transition between elastic and plastic behavior of the pile under stress is not always "clean." This can be understood by using lower and upper bound plasticity. With the shaft, the transition to plastic behavior is fairly abrupt as the bond between the pile and the soil tends to minimize the propagation of further plastic deformation outside of that boundary. Lower and upper bound plasticity can thus be very close. With the toe, plastic behavior generally begins at the outer boundary or radius of the toe and progressively spreads until the toe soil can be said to fail plastically. In these conditions the lower and upper bound conditions vary considerably; the transitional zone from purely elastic to plastic behavior is significant. This obscures a purely elastic solution of the problem.

Softening Coefficients in Clay

Strain-softening coefficients to equate linear shear or elastic modulus with hyperbolic models have been subject of considerable research during the last twenty years. One thing that has emerged is that these coefficients are different for clays than for sands, as is the case with the material factor. For this reason the concentration of this study will be on clay and predominantly clay soils; cohesionless soils need separate consideration.

In any case, probably the most complete study of shear moduli in clay is that of Vardanega and Bolton (2013). They first define a reference strain, thus

$$\gamma_0 = \frac{\tau_{max}}{G_0} \tag{10}$$

which is analogous to the ϵ_0 shown in Figure 1. One thing convenient about clay soils is that, in principle at least, τ_{max} does not vary with intergranular pressure, although in reality this is certainly the case.

The actual shear strain of the soil can be normalized as

$$\gamma' = \frac{\gamma}{\gamma_0} \tag{11}$$

Vardanega and Bolton (2013) performed an extensive study of clay soils and determined that the mean value of γ_0 for a wide range of clay soils was 0.000972 for static loading and 0.001658 for dynamic loading. This is interesting because of the differing response of static and dynamic loading. The entire principle of dynamic testing is that static properties of pile-soil response can be derived from dynamic loading; this variation puts that assumption in a different light.

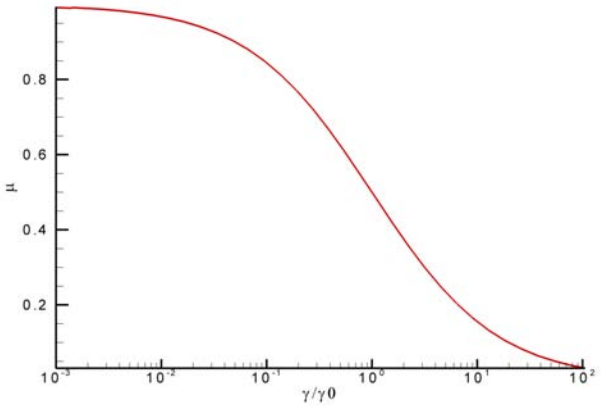

Figure 5. Softening Coefficient vs. Normalized Shear Strain (adapted from Vardanega and Bolton (2013))

Another non-dimensional coefficient that needs to be defined at this point is the hyperbolic softening coefficient itself, which is

$$\mu = \frac{G}{G_0} \tag{12}$$

Using these definitions, and the fact that establishing a reference strain made consolidation of the data practicable, the softening coefficient can be estimated from empirical data as

$$\mu = \frac{1}{1 + \gamma'^{0.736}} \tag{13}$$

This result is plotted in Figure 5. It is very similar to the representation of Figure 2.

Elastic Response of the Shaft Soil and the "Magical Radius"

Probably the single most comprehensive analysis of the problem of elastic shaft friction and pile deflection is that of Randolph and Wroth (1978). Using static equilibrium, the strain at any point at or away from the shaft surface (assuming a round pile) is given by the equation

$$\gamma = \frac{\tau_0 r_0}{Gr} \tag{14}$$

For a constant G, integrating Equation 14 from r_0 to some r_m for displacement yields

$$w_s = \frac{\tau_0 r_0}{G} \ln\left(\frac{r_m}{r_0}\right) \tag{15}$$

Defining

$$r_{rat} = \frac{r_m}{r_0} \tag{16}$$

combining Equations 15 and 16 results in

$$w_s = \frac{\tau_0 r_0}{G} \ln(r_{rat}) \tag{17}$$

Since the piles are (for theoretical purposes) driven into a semi-infinite soil mass, Equation 14 should be integrated to a either $r_m \to \infty$ or thus $r_{rat} \to \infty$. Unfortunately Equation 17 becomes unbounded when this happens. It is necessary to determine what Randolph and Wroth (1978) refer to as a "magical radius," at which point in the soil mass the effects of the pile become insignificant for strain and deflection analysis. Randolph and Wroth (1978) make one estimate of this as

$$r_m = 2L_p\rho(1-\nu) \tag{18}$$

This expression has many assumptions but two need to be mentioned here. The first is that the results are being compared with a finite element analysis where there is a rigid layer at a depth of $2.5L_p$. The second is the inhomogenity factor ρ, which is the ratio of the shear modulus at the midpoint of the pile shaft to that of the toe.

Applying Equation 16 leads to

$$r_{rat} = 4\left(\frac{L_p}{D}\right)\rho(1-\nu) \tag{19}$$

Since it was and is being used in conjunction with a finite element analysis, it should be noted that STADYN uses the pile length as the width of the model and as a depth below the pile toe, which was based on comparison with other FEA models (Warrington (2016).)

Having said this, studies such as Salgado, Loukidis, Abou-Jaoude, and Zhang (2015) indicate that the actual "magical radius" may be considerably lower than that of Randolph and Wroth (1978). This will be revisited shortly but the reduced values of r_m are expressed in Salgado et al. (2015) as a proportion of Randolph and Wroth (1978) values. To do this they use another form of Equation 16 given in Randolph and Wroth (1978), namely

$$r_m = 2.5L_p(1-\nu) \tag{20}$$

which can be reformulated as

$$r_{rat} = 5\left(\frac{L_p}{D}\right)(1-\nu) \tag{21}$$

There are two problems using this formulation.

The first is that it is unlikely that the soil be so homogeneous that $\rho = 1$. If we look at Equation 4, even if all the other parameters (void ratio, softening coefficient, material coefficient) be equal, the result of effective stress variation is that $\rho = \sqrt{2}/2$. Given that the other factors are likely not to be equal, the "Gibson soil" described by Randolph and Wroth (1978), where $\rho = 0.5$, looks to be more realistic.

The second is that the results of Salgado et al. (2015) lead to a yet smaller value for r_{rat} than is given by Equation 21.

Table 1
Magical Radius Ratio for Test Cases

Case	$\frac{L_p}{D}$	r_{rat} from Equation 21, m	Suggested Range of r_{rat}, m
Finno (1989)	33.3	83.3	17-42
Southeast Asia	51	127.6	26-64
Mondello and Killingsworth (2014)	79.8	199.4	40-100

They report that the r_{rat} is more likely 20% to 50% (which itself suggests $\rho = 0.5$) of the results of Equation 21, and they use a value of r_{rat} which is 35% of that result, and suggest that perhaps r_{rat} should be lower than that.

To apply this to the test cases at hand, which are the same as those of Warrington (2016), the parameters which result from Equation 21 are listed in Table 1, assuming for clay $\nu = 0.5$.

In Table 1, the values for L_p/D are taken using the diameter of the pile head. For the first two cases, the pile is uniform. The pile diameter for the last case increases below the pile head, so the value of r_{rat} is even more problematic.

Given the multiple uncertainties surrounding r_{rat}, the best way to proceed is to evaluate the model for a range of values of μ and S and then evaluate those results in light of plausible values of r_m and the resulting homogenized μ that results. Based on Table 1, values of the radius ratio will vary $1 < r_{rat} < 200$.

Homogenized Softening Coefficient for the Pile Shaft

Returning to the evaluation of μ, at this point it is assumed that the maximum shear stress τ_{max} is experienced at the shaft surface (which is a reasonable assumption) and that this stress is at the failure of the soil at the shaft surface. That assumption has limitations (which are the basis of α-methods) but it is a start, as α varies widely in different situations. Using Equation 12 Equation 14 is rewritten for the maximum shear stress at the interface as

$$\gamma = \frac{\tau_{max}}{\mu G_0 r_{rat}} \tag{22}$$

Substituting Equation 10 yields

$$\gamma = \frac{\gamma_0}{\mu r_{rat}} \tag{23}$$

and substituting Equation 11,

$$\gamma' = \frac{1}{\mu r_{rat}} \tag{24}$$

Now solving for μ,

$$\mu = \frac{1}{\gamma' r_{rat}} \tag{25}$$

Equating the right hand sides of Equations 13 and 25 and taking the inverse of both sides, we have at last

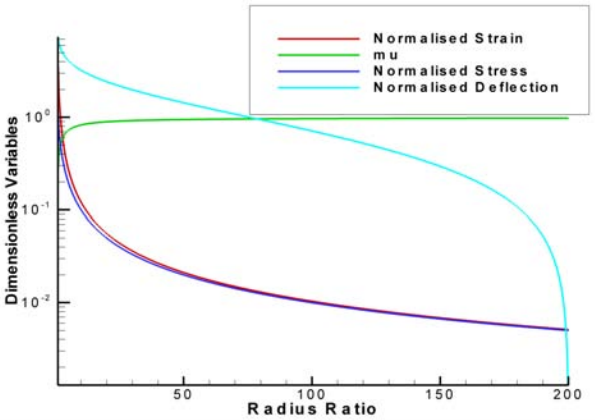

Figure 6. Results for Fixed Value of Magical Radius Ratio

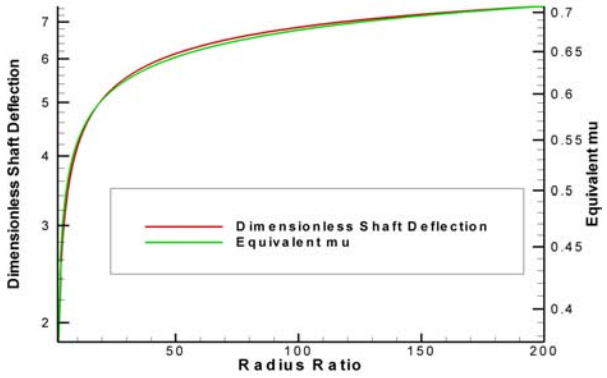

Figure 7. Results for Variable Value of Magical Radius Ratio

$$\gamma' r_{rat} = 1 + \gamma'^{0.736} \tag{26}$$

What we have is a function of normalized strain in clay which varies as the point in the soil is further away from the pile (r_{rat} increases from unity.)

Before the application of Equation 26 is discussed, it is necessary to develop the concept of normalized deflection from normalized strain. Equation 17 is based on a constant value of G (and by extension μ) for all of the uniform soil surrounding the pile shaft. Since Equation 24 is derived from Equation 17, integrating this in the same fashion as we did in Equation 17 yields

$$\bar{w_s} = \frac{1}{\mu} \ln (r_{rat}) \tag{27}$$

Turning back to Equation 26, we can integrate this to the normalized deflection as follows:

1. Determine a suitable r_m and thus r_{rat}. This must be varied, as discussed above.

2. Solve Equation 26 for γ'. The most expeditious method of doing this is numerically. Newton's Method can be used, especially since the derivatives are analytic.

3. Once a range of normalized strains is developed, numerically integrate these strains to a normalized deflection.

The normalized deflection can then be substituted into Equation 27 and a "homogenized" value of μ can be computed which replicates the deflections caused by the strain-varying shear modulus.

With this theory in hand, there are two approaches to analyzing a value for μ. The first is to assume a nominal value for r_{rat} and examine the variation of the properties. The results of this approach for $r_{rat} = 200$ are shown in Figure 6.

The variables plotted are as follows:

- The normalized strain is the solution of Equation 26 at each radius ratio up to the maximum magical radius.
- The normalized stress is the ratio of the shear stress at a given radius to the maximum shear stress at the pile-soil interface.
- The normalized deflection is the integration of Equation 26 assuming that the deflection at the magical radius is zero (the strain obviously is not.)
- The hyperbolic strain softening coefficient is computed by Equation 13.

The following can be deduced from Figure 6:

- The normalized shear stress is approximately 0.5% of its maximum value at the maximum magical radius.
- The normalized shear strain–whose maximum value is 3.53 at the pile surface–is 0.0051 at the magical radius. This is a wider variation than the stress. At this value, following both Figures 5 and 6, the value of $\mu \approx 0.98$. That value exceeds 0.90 at a radius ratio of nearly 22.
- The value of μ at the pile surface is approximately 0.28. This parameter decreases as the pile surface is approached, as expected. This illustrates the hyperbolic softening of the pile material around the shaft that precedes actual plastic deformation; the separation of the two is not something that can be properly represented analytically.
- The normalized deflection at the shaft surface is 7.478. Figure 6 makes clear the effects of forcing this value of zero at the magical radius.

Now it is necessary to analyze the second approach, namely to vary r_{rat} to see how the homogenized value of μ and other parameters vary with it. Given the uncertain nature of r_{rat}, this is the more realistic approach.

Figure 7 shows the results of this approach. Here each radius ratio is actually the r_{rat} at which the dimensionless shaft deflection and equivalent, homogenized μ is evaluated. It is interesting to see that the two variables are nearly proportional to each other. It is also interesting to note that, while the value for homogenized μ increases with r_{rat} as one would expect, it does not "plateau" out. This reflects the unbounded nature of the solution as $r_{rat} \to \infty$.

If we apply the first two test cases on a very rough basis

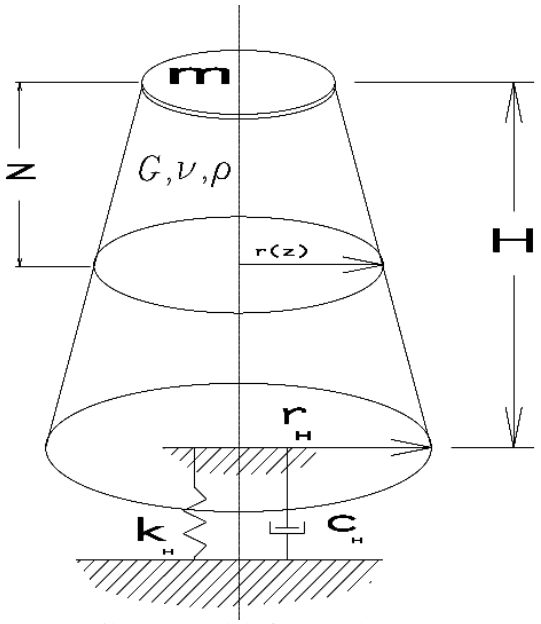

Figure 8. Pile Toe Model (from Holeyman (1988); Warrington (1997))

and apply the reductions of Salgado et al. (2015), plausible values of homogenized $\mu > 0.5$ and can range up to 0.6 and beyond. Given these values and those used in earlier studies, a range of $0.25 \leq \mu \leq 0.7$ will be analyzed, along with all three ranges of S_{bui} proposed earlier.

Homogenized Softening Coefficient for the Pile Toe

The situation at the pile toe is both simpler and more complex than that of the pile shaft.

The model used for the elastic response of the pile toe is that of Holeyman (1988). It models the soil under the toe as the frustrum of a cone, as shown in Figure 8.

The radius of the cone is the same as the pile toe at the toe itself and increases linearly with the depth from the toe. The relationship between the depth z and the radius is given by the equation

$$r(z) = r_t + 1.085(1-\nu)z \tag{28}$$

Since the stress is uniaxial and is proportional to the cross-sectional area, the ratio of the stress at the pile toe and at some point z below the pile toe is given as

$$\frac{\sigma_z}{\sigma_t} = \frac{r_t^2}{(r_t + 1.085(1-\nu)z)^2} \tag{29}$$

or

$$\frac{\sigma_z}{\sigma_t} = \frac{1}{\left(1.085(1-\nu)\frac{z}{r_t} + 1\right)^2} \tag{30}$$

For uniaxial stress, $\sigma = 2\tau$, and so, with additional rearrangement,

$$\tau_z = \frac{\tau_t}{\left(1.085(1-\nu)\frac{z}{r_t} + 1\right)^2} \tag{31}$$

By analogy to Equation 14,

$$\gamma_z = \frac{\tau_t}{\mu G_0 \left(1.085(1-\nu)\frac{z}{r_t} + 1\right)^2} \tag{32}$$

and finally, in a similar way to Equation 24,

$$\gamma' = \frac{1}{\mu} \frac{1}{\left(1.085(1-\nu)\frac{z}{r_t} + 1\right)^2} \tag{33}$$

If we define

$$z' = \frac{z}{r_t} \tag{34}$$

Equation 33 becomes

$$\gamma' = \frac{1}{\mu(1.085(1-\nu)z' + 1)^2} \tag{35}$$

As was the case with the shaft, there are two possible solutions. The first is to assume a uniform, homogenized value of μ and compute a normalized value for the toe deflection. To do this it is necessary to integrate Equation 35 to some magical depth ratio (corresponding to the magical radius of the shaft.)

$$\bar{w_s} = \frac{z'}{\mu(1 + 1.085(1-\nu)z')} \tag{36}$$

or, solving for μ,

$$\mu = \frac{z'}{\bar{w_s}(1 + 1.085(1-\nu)z')} \tag{37}$$

The other solution is to combine Equation 13 and Equation 35 and eliminate μ, which yields

$$\gamma'(1 + 1.085(1-\nu)z')^2 - 1 - \gamma'^{0.736} = 0 \tag{38}$$

This equation was then numerically integrated in the same way as the shaft for various values of z' to obtain values of $\bar{w_s}$, which were then applied to Equation 37 to obtain values of homogenized μ.

Analogous to Figure 6 is Figure 9 for the toe.

The whole concept of a "magical depth ratio" is not as critical with the toe as it is with the shaft because the solution of Equation 35 as γ' decreases with the square of z' rather than linearly. The value of $z'_{max} = 200$, carried over from the shaft resistance, is reasonable in this case. Nevertheless the values for μ approach unity for increasing values of z'.

When the depth ratio is varied, the results are as shown in Figure 10.

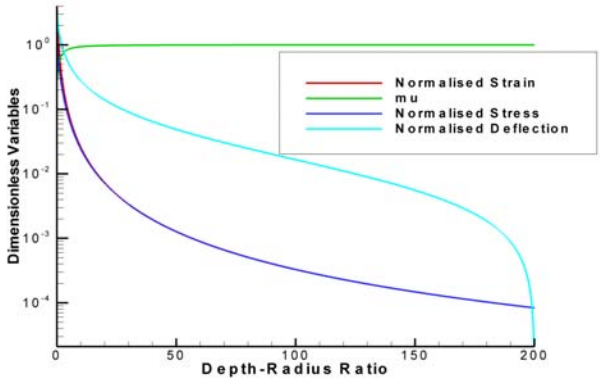

Figure 9. Results for Fixed Value of Magical Depth Ratio

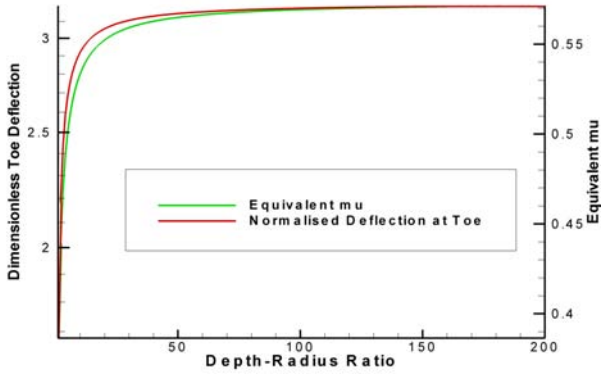

Figure 10. Results for Variable Value of Magical Depth Ratio

For the toe both the equivalent μ and the normalized deflection come to a more definite maximum value than they do with the shaft. The homogenized value of μ peaks at just above 0.57, which is in the same order of magnitude as the range of shaft softening coefficients estimated earlier.

This definite result, however, should be tempered by considerations of the interaction of elastic and plastic phenomena. This is where the toe is more complex in its interaction with the soil than the shaft. With the shaft, the initial plastic failure takes place at or near and along the pile-soil interface. The lower and upper bounds of plasticity are very close. With the toe, failure is more progressive (van Baars (2016).) Lower and upper bounds are separated (as they are with, say, classic bearing capacity failure) and there is a portion of the failure history where elastic and plastic stress and strain are taking place simultaneously.

Given all of this, it was decided to force the shaft and toe softening coefficients to be the same for the range of coefficients tested. This may be subject to subsequent adjustment but given the values we have it is probably a reasonable assumption.

Results of STADYN Analysis

All of this was applied to the STADYN program, which was originally described by Warrington (2016) and updated by Warrington and Newman (2018). Since the latter revision the following changes to the program have taken place:

- The method by which the modulus of elasticity/shear modulus has been changed, first through the adaptation of the Hardin and Black (1968) model and then by the adaptation of the Bui et al. (2010) void ratio/porosity model. These changes were described in detail earlier and provide the basis for the current study. In both cases the dry unit weight computation and cohesion were altered as well.
- The cohesion of the soil at the pile shaft-soil interface has been altered to reflect the effects of that interface on the apparent strength of the soil, in accordance with the results of Kolk and van der Velde (1996). In addition to the changes in the shaft surface cohesion, this also changed the value of ν. For cohesionless soils the value of ν was changed to replicate the lateral pressures implied by the method of Randolph et al. (1994), but for this study computation of ν using Jaky's Equation was reverted to because of uncertainties in N_q. These can be resolved using field data but due to the nature of the model incorporating this kind of data is problematic.
- Provision for a cushion (hammer and/or pile) coefficient of restitution was included. This was to make forward runs which included a hammer more realistic.

The test cases are noted in Table 1.

Results from Finno (1989) Case

This case is, in many ways, the most satisfactory of the three cases, because it has both static and dynamic test data (although it lacks dynamic monitoring data during driving.) The soils the pile is being driven into are mostly (but not entirely) cohesive.

The simplest way to compare the results is through the Davisson Capacity results that come from the static loading test. These are presented in Figure 11.

The results show consistent patterns, which can be explained as follows:

1. The Davisson capacity of the pile increases in all cases with an increase in μ, which is roughly proportional to the increase of shear or elastic modulus in the soil. As an example, doubling the value of μ from $\mu = 0.25$ to $\mu = 0.5$ for values of minimum $S_{bui} \geq 100$ results in an increase in Davisson capacity ranging from 11-14%. The one exception are the capacities for the low values of μ coupled with the minimum $S_{bui} = 50$, which are below the linear pattern of the other values of S_{bui}.

2. The four values of minimum S_{bui} are doubled from the one below it. In each case, doubling that value increased

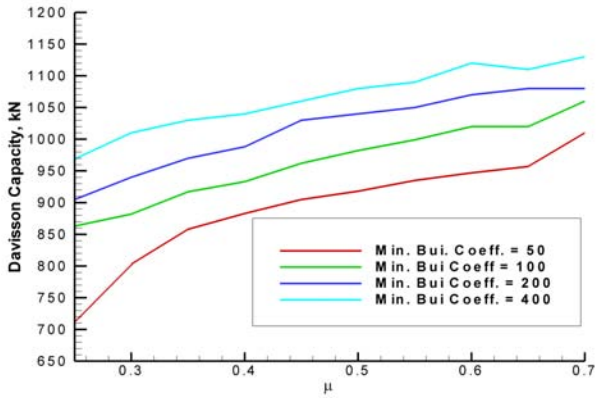

Figure 11. Davisson Capacity Results from Finno (1989) Case

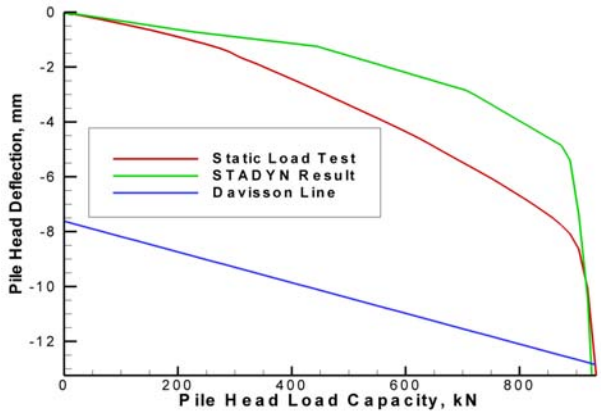

Figure 12. Comparison of STADYN Static Results with Static Load Test for Finno (1989)

mean value of the Davisson capacity by about 5%, the fall-off for $S_{bui} = 50$ excepted.

3. All of these results indicate that the assumed value of G, be it from varying S or μ, is an important component in estimating the Davisson capacity of the pile, although the single most important factor is the maximum shear at the pile interface.

One case with a very close Davisson capacity result to the original load test was the case for $S_{bui} = 50$ and $\mu = 0.55$, and the comparison between the STADYN and static load results is shown in Figure 12.

The results obviously show good agreement with the static load test at Davisson failure but show that the STADYN model is stiffer before that point. This is a characteristic of the model that requires improvement.

Results from Southeast Asia Case

Although this case is essentially theoretical, it is of special interest for this study because the soils are entirely cohesive, and this study focuses on clays.

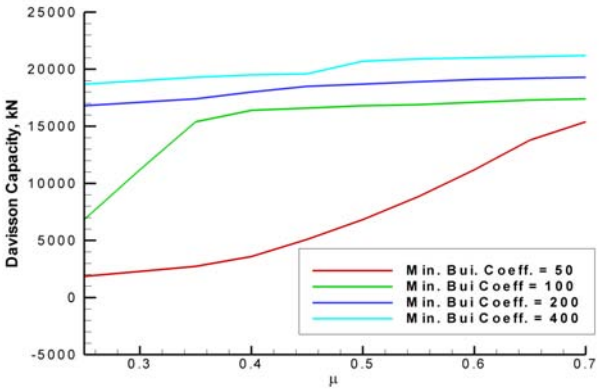

Figure 13. Davisson Capacity Results from Southeast Asia Case

Running a similar array of test cases as before, the results are presented in Figure 13.

The cases of minimum $S_{bui} = 200$ and minimum $S_{bui} = 400$ show the same regular pattern as their counterparts in Figure 11. The results for minimum $S_{bui} = 100$ have a fall-off for lower values of μ. The important outlier in the results–albeit without model collapse–are those for minimum $S_{bui} = 50$, which curve upward from a low Davisson capacity, not quite linearizing even at $\mu = 0.7$. One important change in the STADYN model was that the values of cohesion at the pile-soil interface were reduced according to the correlation of Kolk and van der Velde (1996). Using that method, the static capacity of the pile (assuming $N_q = 9$ for the toe, whose resistance is minimal) is 15,739 kN. This capacity is arrived at for minimum $S_{bui} = 100$ at $0.35 < \mu < 0.4$, in which region the capacity variation becomes approximately linear. Since, as discussed earlier, the effective value of μS can be made constant by proportionally varying μ and S, one would expect this to take place for $S_{bui} = 50$ at $0.7 < \mu < 0.8$.

Results from Mondello and Killingsworth (2014) Case

This case, the only inverse case in Warrington (2016), is especially interesting because of the structure of Equation 4. With the forward cases, μ and S_{bui} are specified as program inputs. Here the value of μ is given and the program varies S_{bui} through the soil properties to give an optimum signal match. In this way the program effectively determines the product of the two parameters. The results of this will show if the pile capacity it in fact a result of the product of the two and independent of each individually or not.

To accomplish this, as with the other two cases, the same array of combinations of μ and S_{bui} was applied to this case as well. Two results were tracked: the Davisson capacity results (as with the forward cases) and the least squares signal difference. One challenge this case has always had is that,

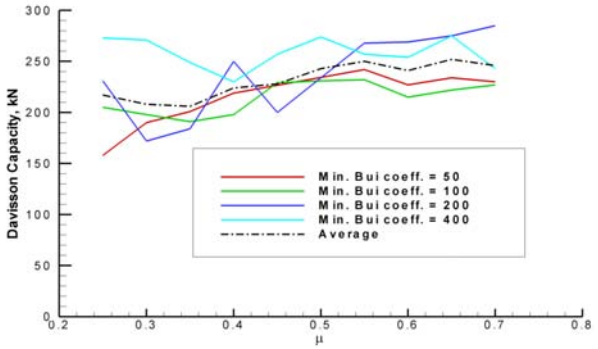

Figure 14. Davisson Capacity Results for Mondello and Killingsworth (2014) Case

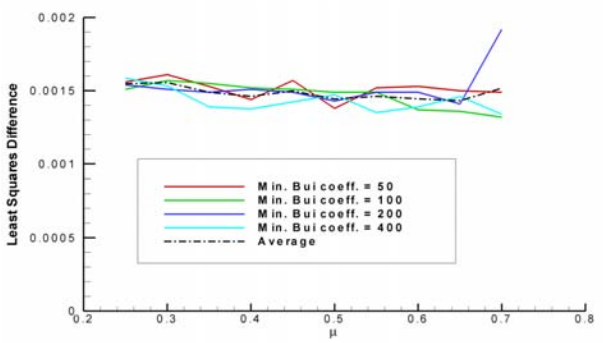

Figure 15. Least-Squares Signal Difference Results for Mondello and Killingsworth (2014) Case

since the soils are so soft and the deflections (both static and dynamic) are so large, the possibility of model collapse is greater than normal. With the signal difference, only in one case ($\mu = 0.7$, *minimum* $S_{bui} = 200$) did a significant outlier in the data result, and so all of the results were included in the data analysis. With the Davisson capacity, several of the cases resulted in outlier results, and these data points were excluded from the analysis. They are as follows, for minimum values of S_{bui}:

- $\mu = 0.25$, $S_{bui} = 100$
- $\mu = 0.45$, $S_{bui} = 50$
- $\mu = 0.5$, $S_{bui} = 50$ & $S_{bui} = 200$
- $\mu = 0.7$, $S_{bui} = 100$

It should be noted that, for ranges of $0.3 \leq \mu \leq 0.4$ and $0.55 \leq \mu \leq 0.65$, there were no outliers in the data, even with the wide range of inputs for minimum values of S_{bui}.

The Davisson capacity results are shown in Figure 14. These results show that, for increasing values of μ, there is a general upward trend in the capacity, although there is also a "flattening out" of the capacity increase in the higher values of μ. Capacity also tends to increase for increasing values of S_{bui} once the minimum $S_{bui} > 100$.

The results for least squares signal difference are shown in Figure 15.

Even when the outlier is retained (as it was not for the Davisson capacity,) the results for this parameter are more consistent than with Davisson capacity. Increasing μ resulted in a general downward trend for least-squares signal differences.

Discussion

1. The results for the higher minimum values of S_{bui} are probably not realistic. Studying these variations, however, is interesting because they show that, although shear modulus is an important parameter in pile capacity based on settlement, it is not the most important factor. For example, with the Finno (1989) case, for most values of μ the Davisson capacity did not increase more than 20% with an eight-fold increase in S_{bui}. The results for the Southeast Asia case were complicated by the low values of Davisson capacity for the minimum $S_{bui} = 50$, but for the others a similar trend as the Finno (1989) case was noted.

2. Although the results of Salgado et al. (2015) allow for modification of the values of the magical radius r_m, variations in the formulation of this parameter in Randolph and Wroth (1978) need to be taken into consideration. Defining this parameter properly is critical in modeling the pile in anything other than a purely one-dimensional formulation.

3. One thing that was not attempted was the modification of the STADYN model's modeled soil size to fit the magical radius. Changing this configuration must be done with care as STADYN is both a static and a dynamic model. While the static model can be sized to include the soil are which is anticipated to be stressed, the dynamic model must be large enough to prevent reflections of the waves induced in the soil during impact to return to the pile and thus interfere with the results. This is because STADYN uses a rigid, Dirichlet boundary, and is intended to be large enough to eliminate reflected waves back on the pile.

4. The application of elastic theory, modified by hyperbolic softening, shows that higher values of μ are indicated. By "higher" this means 0.6-0.7 for the shaft and 0.55-0.6 for the toe. It should be reiterated that the same value for μ for the shaft and toe was used throughout this analysis. Comparison of the elastic analysis for the shaft and toe shows that, while the maximum values are similar, they are not identical; the unbounded nature of the shaft results allows for higher values of μ. Given the uncertainties discussed earlier, separating these values of μ may result in values that are more precise than accurate.

5. Within the limitations of the results, this conclusion was borne out in the results from the STADYN model, especially when the minimum $S_{bui} = 50$ is used. The results shown in both Figures 12 and 13 indicate that the higher values of μ are more consistent with the static load test data or the static results. For the Mondello and Killingsworth (2014) case, the lower values of the least squares differences

for higher values of μ indicate that these results at are more realistic.

6. Hyperbolic strain softening of soils is an important topic that is gaining prominence in practice. Implementation of the results of these studies would be significantly furthered by uniform notation, a more universally agreed on value for $F(e)$, and empirical formulations that are dimensionally consistent in formulation to allow their use in more than one system or set of units.

Conclusions

1. At this point a reasonable model to estimate suitable values of μ for clay has been established. This should be seen a framework of analysis and not a definitive conclusion; many more test cases and analytical work remains before such a conclusion (to the extent possible in geotechnical engineering) can be established. For purposes of further use of the STADYN model, a value of $\mu = 0.65$ will be used.

2. Further studies are necessary for the behavior of sands, which may either result in modifying this value for all cases or establishing a separate values for sands.

3. The values used for shear moduli in one-dimensional models such as Randolph and Simons (1986) needs to be re-examined in view of the effects of hyperbolic strain softening. Such revisiting may in fact make these simpler models more viable in actual application.

Nomenclature

α Clay Pile-Soil Interface Coefficient

$\bar{n}$ Effective Stress Function Exponent

$\bar{w_s}$ Normalized Pile Displacement

ϵ Normal Strain

ϵ_0 Reference Normal Strain

ϵ_1 Normal Strain at Linear Failure Stress

γ Shear Strain

γ' Normalized Shear Strain

γ_0 Reference Shear Strain

μ Hyperbolic strain softening coefficient

ν Poisson's Ratio

ρ Shear Modulus Ratio

σ_1 First Principal Stress, kPa

σ_2 Second Principal Stress, kPa

σ_3 Third Principal Stress, kPa

σ_0 Deviatoric Stress, kPa

σ_t Stress at pile toe, kPa

σ_z Stress at some point z below pile toe, kPa

τ_0 Shear Stress at Pile Shaft Interface, kPa

τ_{max} Maximum Shear Stress, kPa

ξ, η Dimensionless Soil Coefficients for STADYN

a, b Hyperbolic Coefficients

D Diameter of pile, m

E Elastic Modulus, kPa

e Void Ratio

E_{ti} Small-Strain Elastic Modulus, kPa

$F(e)$ Voic Ratio Function

$F(n)$ Porosity Function

G Shear Modulus of Elasticity, kPa

G_0 Small-Strain Shear Modulus of Elasticity, kPa

L_p Length of pile, m

n Porosity

p_{atm} Atmospheric Pressure at Sea Level, kPa

r Radius From Pile Center, m

$r(z)$ Radius of Pile Toe Influence Cone, m

r_0 Pile Outside Radius, m

r_m Magical Radius, m

r_{rat} Magical Radius ratio

r_t Radius of Pile Toe, m

S Material Factor for Shear Modulus

S_{bui} Material Factor for Bui correlation

$S_{H\&B}$ Material Factor for Hardin and Black correlation

w_s Deflection at Pile Surface, m

z Depth from pile toe, m

z' Ratio of depth under pile toe to pile toe radius

References

Bui, M., Clayton, C., & Priest, J. (2010, May). The universal void ratio function for small strain shear modulus. *Fifth Int. Conf. on Recent Advances in Geotechnical Earthquake Engineering and Soil Dynamics*, *29*(1).

Duncan, J. M., & Chang, C.-Y. (1970, September). Nonlinear analysis of stress and strain in soils. *Journal of the Soil Mechanics and Foundations Division*, *96*(SM5), 1629–1653.

Finno, R. (1989). *Predicted and observed axial behavior of piles: Results of a pile prediction symposium*. New York, NY: American Society of Civil Engineers.

Hardin, B. O., & Black, W. (1968, January). Vibration modulus of normally consolidated clay. *Journal of the Soil Mechanics and Foundations Division*, *94*(2), 353–369.

Holeyman, A. (1988, May). Modeling of dynamic behavior at the pile base. *Proceedings of the Third International Conference on the Application of Stress-Wave Theory to Piles*.

Kolk, A., & van der Velde, A. (1996, May). A reliable method to determine friction capacity of piles driven into clays. *Proceedings of the 28th Offshore Technology Conference,*, OTC 7993.

Loehr, J., Lutenegger, A., Rosenblad, B., & Boeckmann, A. (2016). *Geotechnical site characterization: Geotechnical engineering circular no. 5* (No. FHWA NHI-16-072). Washington, DC: Federal Highway Administration.

Mondello, B., & Killingsworth, S. (2014). *Dynamic pile testing results, Crescent Foundation demonstration test pile – Vulcan SC9 hammer, Kenner, Louisiana* (Tech. Rep.).

Randolph, M., Dolwin, J., & Beck, R. (1994). Design of driven piles in sand. *Geotechnique*, *44*(3), 427–448.

Randolph, M., & Simons, H. (1986). An improved soil model for one-dimensional pile driving analysis. *Numerical Method in Offshore Piling*, 3–18.

Randolph, M., & Wroth, C. (1978, December). Analysis of deformation of vertically loaded piles. *Journal of the Geotechnical Engineering Division*, *104*(GT12).

Salgado, R., Loukidis, D., Abou-Jaoude, G., & Zhang, Y. (2015). The role of stil stiffness non-linearity in 1d pile driving simulations. *Geotechnique*, *65*(3), 169–187.

van Baars, S. (2016, May). The influence of the shaft friction and pile shape on the pile tip bearing capacity. *Proceedings of the 17 th Nordic Geotechnical Meeting Challenges in Nordic Geotechnic*, 711–717.

Vardanega, P., & Bolton, M. (2013, September). Stiffness of clays and silts: Normalizing shear modulus and shear strain. *Journal of Geotechnical and Geoenvironmental Engineerins*, *139*, 1575–1589.

Warrington, D. C. (1997). *Closed form solution of the wave equation for piles* (Unpublished master's thesis). University of Tennessee at Chattanooga, Chattanooga, TN.

Warrington, D. C. (2016). *Improved methods for forward and inverse solution of the wave equation for piles* (Unpublished doctoral dissertation). University of Tennessee at Chattanooga, Chattanooga, TN.

Warrington, D. C., & Newman, J. C. (2018, March). Inverse method for pile dynamics using a polytope method. *Presented at the International Foundations Congress and Equipment Expo*.

Yang, J. (2006, September). Influence zone for end bearing piles in sand. *Journal of Geotechnical and Geoenvironmental Engineering*, *132*(9).